



## A Cost Effective Green Biosorbent *Simarouba glauca* Seed Shell for Removal of Rhodamine B from Aqueous Solutions

B. JEYAGOWRI<sup>1,\*</sup> and R.T. YAMUNA<sup>2</sup>

<sup>1</sup>Department of Chemistry, Hindusthan College of Engineering and Technology, Coimbatore-641 032, India

<sup>2</sup>Department of Chemistry, Kalaingar Karunanidhi Institute of Technology, Coimbatore-641 402, India

\*Corresponding author: E-mail: gowrivasuphd2010@gmail.com

Received: 19 September 2014;

Accepted: 4 December 2014;

Published online: 17 March 2015;

AJC-17012

This study presents the potential feasibility of a low cost green biosorbent for the removal of a basic dye rhodamine B from aqueous solutions. The biosorbent were characterized by FT-IR, SEM, XRD, BET and CHNS analysis. The effect of various parameters like initial dye concentration, contact time, pH and adsorbent dose were investigated in batch mode. The equilibrium data was analyzed using Langmuir, Freundlich, Temkin and D-R isotherm models. Equilibrium data showed best fit for Langmuir isotherm with maximum adsorption capacity 11.63 mg/g. Four kinetic models pseudo first order, pseudo second order, intraparticle diffusion and Boyd model were employed to describe the adsorption mechanism. Adsorption kinetics followed pseudo second order model with the coefficient of correlation  $R^2 = 1$ . The experimental results suggested that SFTS (a biosorbent) was an excellent sorbent for removal of rhodamine B from aqueous solution.

**Keywords:** Biosorption, *Simarouba glauca* seed shell, Rhodamine B, Adsorption isotherm, Kinetic studies.

### INTRODUCTION

Rapid industrialization and urbanization causes significant increase in release of harmful toxic pollutants to the natural environment. The most easily recognizable pollutants in environment are coloured dyes used in various textile and paper industries. Synthetic dyes are common water pollutants due to their high solubility. The discharge of dye bearing wastewater into natural streams and rivers not only deteriorates the water quality, but also have significant impact on human health due to toxic, carcinogenic, mutagenic or teratogenic effects. Therefore, removal of dyes from waste water becomes necessary and important. The most common conventional methods for removal of dyes in wastewater are physical, chemical and biological methods. Chemical methods such as coagulation or flocculation to remove dyes are not effective for highly soluble dyes. Biological methods are not effective in removal of dyes on continuous basis and longer time is required for decolorization - fermentation processes. Physical methods such as ion - exchange, membrane filtration, electrochemical destruction etc are widely used but are found to be costlier and lead to generation of sludge and by products<sup>1</sup>. Recent research activities are focused on biosorption, a powerful alternative for removal of dyes and heavy metals from industrial waste water. Biosorption has the major advantages of low cost, high efficiency, minimization of chemical or biological sludge,

regeneration of biosorbent and possibility of sorbate recovery over other conventional methods<sup>2</sup>. The agricultural waste products have a great potential as biosorbents for removal of dyes from aqueous solutions. Some of the low cost biosorbents reported in literature include papaya seeds<sup>3</sup>, sunflower hulls<sup>4</sup>, tamarind fruit shell<sup>5</sup>, ginger waste<sup>6</sup>, coir pith<sup>7</sup>, citrus waste<sup>8</sup>, neem saw dust<sup>9</sup>, Jute stick powder<sup>10</sup>, green pea peels<sup>11</sup>, milled sugarcane bagasse<sup>12</sup>.

*Simarouba glauca*, commonly known as paradise tree is an edible oil seed bearing tree well suited for warm, humid and tropical regions. This eco-friendly tree with well developed root system and with evergreen dense canopy efficiently checks soil erosion, supports soil microbial life and improves ground water position. The seed contains about 50-60 % oil with 63 % unsaturated fatty acid among which 59.1 % is oleic acid and is fit for human consumption. The seed shell, a waste product from this eco friendly tree has been used for the present study for the removal of rhodamine B from aqueous solutions. The main objective of the present study is to investigate the potential feasibility of formaldehyde treated *Simarouba glauca* seed shell in the removal of rhodamine B from aqueous solutions.

### EXPERIMENTAL

Rhodamine B is a cationic dye, purchased from SD Fine Chem Limited, Mumbai, The structure of dye is shown in Fig. 1. The absorbance maximum is 547 nm.

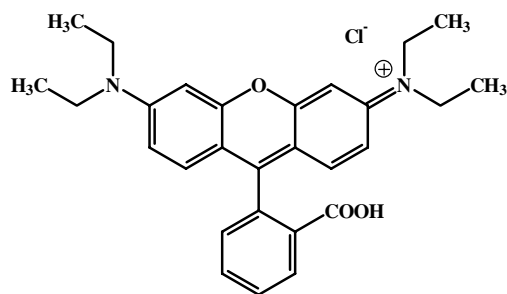


Fig. 1. Structure of Rhodamine B

**Preparation of adsorbent (SFTS):** The seed shells were powdered and were steam activated for 40 min. and then washed well with distilled water. The washed material was then treated with 1 % formaldehyde in the ratio 1:5 and was heated in hot air oven at 50 °C for 4 h. The seed shell powder was filtered, washed again with distilled water to remove free formaldehyde and activated at 80 °C in hot air oven for 24 h. The treated material (SFTS) was sieved for the particle size 75-150 µm and stored in an air tight plastic container for further use.

**Characterization of adsorbent:** The surface functional groups of the adsorbent SFTS were detected using Fourier transform infrared spectrometer (Shimadzu, model IRAffinity-1). The samples were prepared as KBr pellets and scanned in the range of 4000-400 cm<sup>-1</sup>. The scanning electron microscopy (SEM, JSM-6390, JOEL) was carried out to study the surface texture and morphology features of the adsorbent. The Brunauer-Emmett-Teller (BET) surface area, total pore volume and pore size distribution were determined by nitrogen sorption at 77 K (Micromeritics, ASAP 2010). Elemental Vario EL III was used for elemental analysis of the adsorbent. The structural characterization was also done using X-ray diffraction studies.

**Determination of zero point charge (pH<sub>zpc</sub>) of SFTS:** The process of adsorption is greatly influenced by the pH of the solution. The pH of the solution affects the surface charge of adsorbent as well as the degree of ionization of different pollutants<sup>13,14</sup>. The influence of pH on the adsorption process can be described using zero point discharge (pH<sub>zpc</sub>), the point at which the net charge of adsorbent is zero<sup>13</sup>. The zero point charge is determined by carrying out experiments in a series of 250 mL conical flasks containing 50 mL of 1 × 10<sup>-3</sup> M NaNO<sub>3</sub> and 0.1 g of adsorbent (SFTS). The pH values were adjusted between 3-11 using 0.1 M HCl and 0.1 M NaOH. The initial pH of the solution was measured and then 1.912 g of NaNO<sub>3</sub> is added to each sample and allowed for equilibration. The final pH was also measured. The difference between initial pH and final pH (ΔpH) values were plotted against initial pH. The point of intersection of curve at ΔpH = 0 give the pH<sub>zpc</sub><sup>15</sup>.

**Batch mode studies:** The batch mode adsorption studies were carried out to study the effect of parameters like initial concentration and time, adsorbent dosage, pH for the removal of rhodamine B dye. Batch adsorption experiments were carried by adding 0.1 g of SFTS into 250 mL Erlenmeyer flasks containing 50 mL of different initial concentrations (5, 10, 20 and 30 mg/L) of rhodamine B solution. The flasks were agitated in a rotary shaker at room temperature until equilibrium was

reached. The adsorbent was separated by filtration and the concentration of rhodamine B in supernatant was determined at a wavelength of maximum adsorption (λ<sub>max</sub>) at 547 nm by visible spectrophotometer (Shimadzu Visible Spectrophotometer UVmini-1240 V). The amount of adsorbed dye at equilibrium q<sub>e</sub> (mg/g) and the removal percentage were calculated by the following equations:

$$q_e = (C_0 - C_e) V / W \quad (1)$$

$$\% \text{ removal} = ((C_0 - C_e) / C_0) \times 100 \quad (2)$$

where C<sub>0</sub> and C<sub>e</sub> are the initial and equilibrium concentrations of dye, respectively (mg/L). V is the volume of dye solution (l) and W is the weight of adsorbent used (g).

## RESULTS AND DISCUSSION

**Structural characterization studies:** The FT IR spectra of adsorbent SFTS were taken before and after dye adsorption (Fig. 2.). The broad and intense band at 3356 cm<sup>-1</sup> corresponds to O-H stretching vibrations. The band at 2935 cm<sup>-1</sup> represents symmetric or asymmetric C-H stretching vibration of aliphatic acids. The bands at 1616 and 1516 cm<sup>-1</sup> reveal the aromatic C-C stretching in phenyl ring of lignin. The absorption band at 1450 cm<sup>-1</sup> is assigned to methoxy group of lignin<sup>16,17</sup>. A weak absorption band at 1722 cm<sup>-1</sup> corresponds to C=O stretching of -COOH group. The FTIR spectrum well indicates the presence of hydroxyl and carbonyl groups in SFTS. The disappearance of peak at 1722 cm<sup>-1</sup> and shifting of peaks confirms the involvement of functional groups in SFTS in adsorption process. The X-Ray diffractogram of SFTS (Fig. 3a) with sharp peaks confirms the crystalline nature of the adsorbent. The disappearance of these sharp peaks in X-Ray diffractogram of dye loaded adsorbent (Fig. 3b) confirms the effective adsorption of dye molecules onto adsorbent surface. The elemental analysis of SFTS was also done and the composition is shown in Table-1.

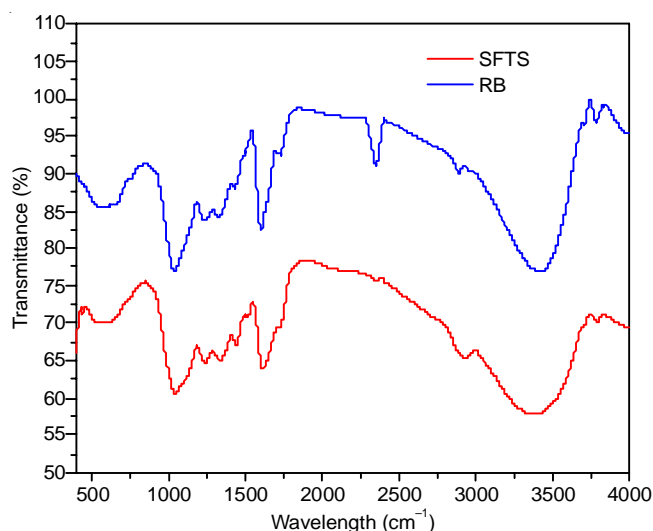


Fig. 2. FT-IR spectrum of SFTS before (SFTS) and after adsorption (RB)

**Surface morphological studies:** Fig. 4a and 4b show the surface morphology of the adsorbent SFTS and dye loaded SFTS. It is clearly seen from Fig. 4a that the surface is uneven, rough and porous. The SEM image of dye loaded SFTS clearly shows the adsorption of dye molecules on to the adsorbent surface. The BET surface area, total pore volume and average

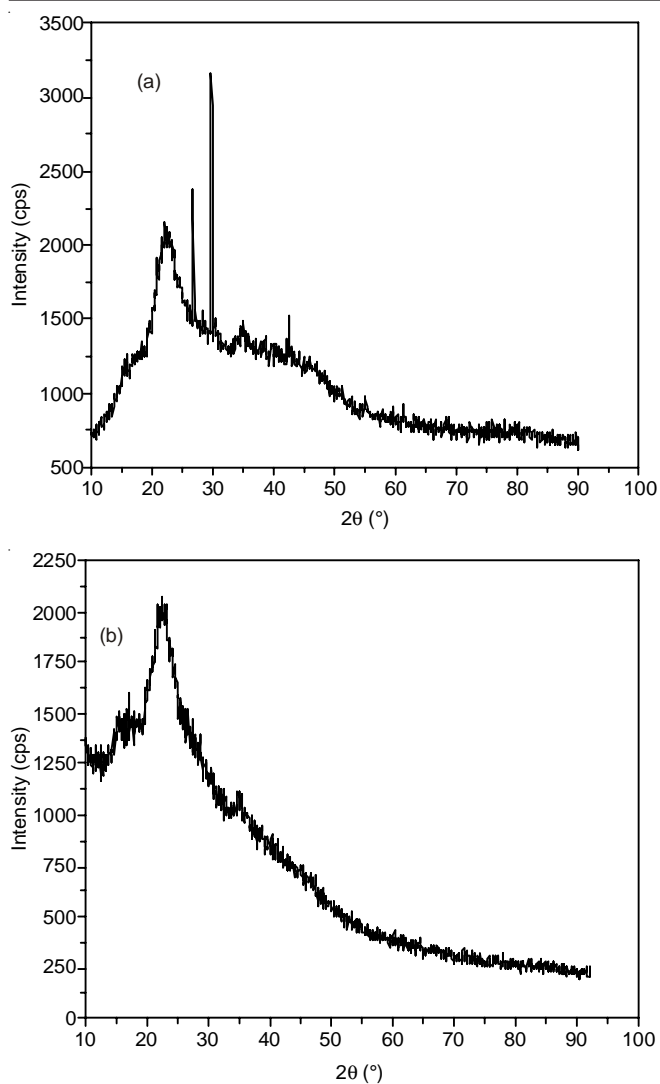


Fig. 3. X-ray diffraction pattern of SFTS (a) before adsorption (b) after adsorption

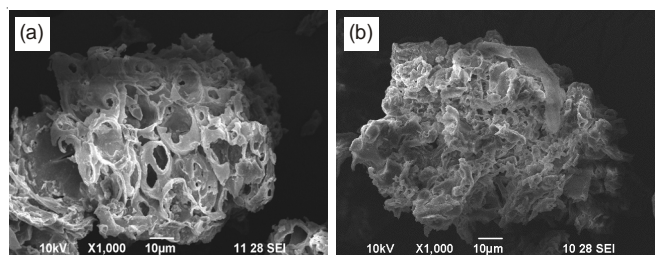


Fig. 4. SEM image of SFTS (a) before adsorption and (b) after adsorption

pore diameter of SFTS were given in Table-1. The pore size distribution of SFTS is shown in Fig. 5. It is seen from the figure that most pores of SFTS are in the mesoporous range (diameter 2-50 nm)<sup>18</sup>. The average pore diameter of SFTS (Table-1) confirms the mesoporous nature of SFTS.

**Zero point discharge ( $pH_{zpc}$ ):** The  $pH_{zpc}$  of SFTS is found to be 3.8. When the pH of the solution is less than  $pH_{zpc}$ , the surface of the adsorbent becomes positively charged and the concentration of  $H^+$  ions increases which competes with the dye cations causing decrease in dye uptake. The surface of adsorbent becomes negatively charged at  $pH > pH_{zpc}$  and favors uptake of cationic dyes due to increased electrostatic force of attraction.

TABLE-1  
PHYSICOCHEMICAL CHARACTERIZATION OF SFTS

Parameters	Values
BET surface area ( $m^2/g$ )	1.8704
Total pore volume ( $cm^3/g$ )	0.003948
Average pore diameter (nm)	8.4422
Point of zero charge (pH zpc)	3.8
C (%)	52.21
H (%)	7.07
N (%)	1.32
S (%)	0.32

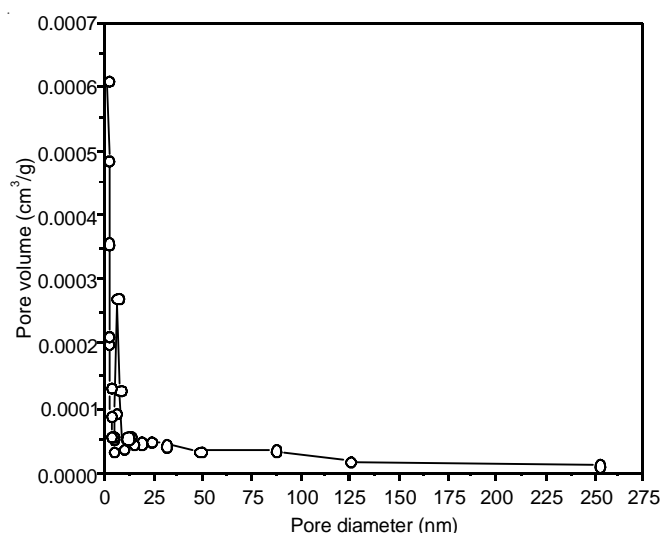


Fig. 5. Pore size distribution of SFTS

**Effect of initial concentration and time:** The effect of initial concentration of rhodamine B on the rate of dye bio-sorption onto SFTS was studied at constant SFTS concentration (0.1 g/50 mL) and at different initial rhodamine B concentration (5, 10, 20 and 30 mg/L) for different time intervals from 5 to 180 min. at room temperature.

The adsorption of rhodamine B *versus* contact time at different initial concentrations is shown in Fig. 6. It is seen from Fig. 6 that the actual amount of dye adsorbed per unit mass of adsorbent increased with increase in rhodamine B concentration. This is probably due to the fact that higher initial concentration enhanced the driving force between the aqueous and solid phases and increased the number of collisions between dye ions and adsorbents.

The adsorption capacity for rhodamine B at equilibrium increased from (2.28, 4.50, 7.7 and 10.6 mg/g), respectively as rhodamine B concentration increased from (5, 10, 20 and 30 mg/L). It is evident from Fig. 6 that the contact time needed for rhodamine B solutions with initial concentration of 5-30 mg/L to reach the equilibrium was 80 min. After equilibrium time of 80 min, the concentration of rhodamine B in liquid phase remained almost constant.

**Effect of pH:** The pH of the dye solution is one of the most important parameter as the protonation of functional groups on biosorbent surface and the chemistry of dye molecules are strongly affected by pH of the solution.

The effect of initial pH on the adsorption of rhodamine B by SFTS was studied by varying the pH of dye solution from 2 to 11 for initial concentration of 40 mg/L. (Fig. 7). It is

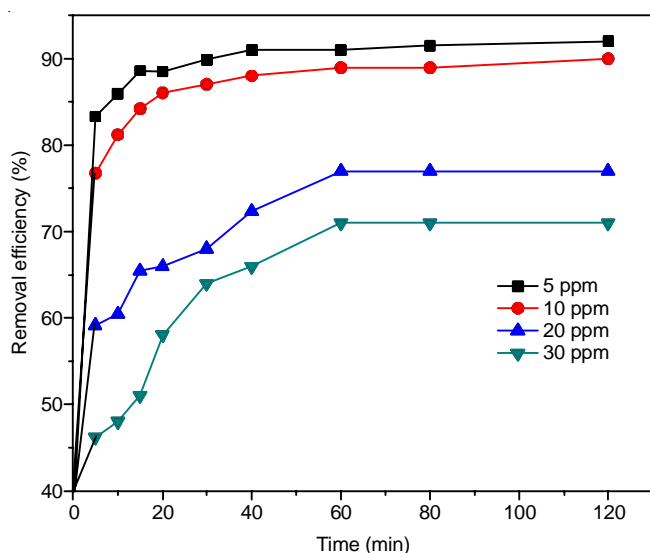


Fig. 6. Effect of contact time on adsorption of rhodamine B onto SFTS (adsorbent dose = 0.1 g/50 mL)

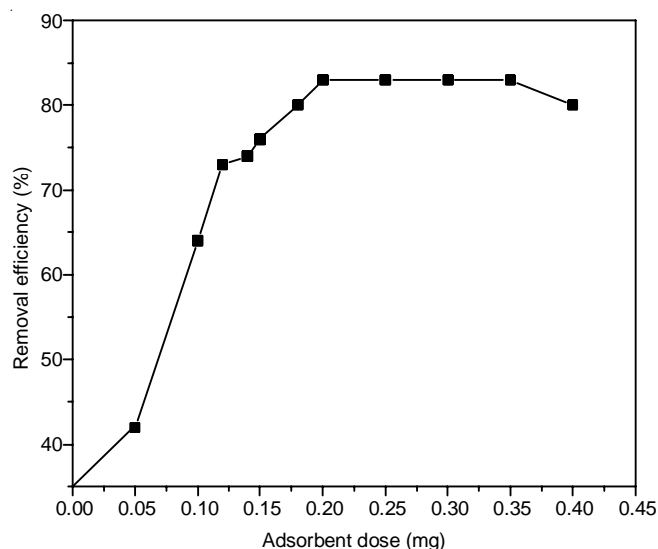


Fig. 8. Effect of adsorbent dose on adsorption of rhodamine B onto SFTS (V = 50 mL, initial concentration = 40 mg/L, t = 80 min)

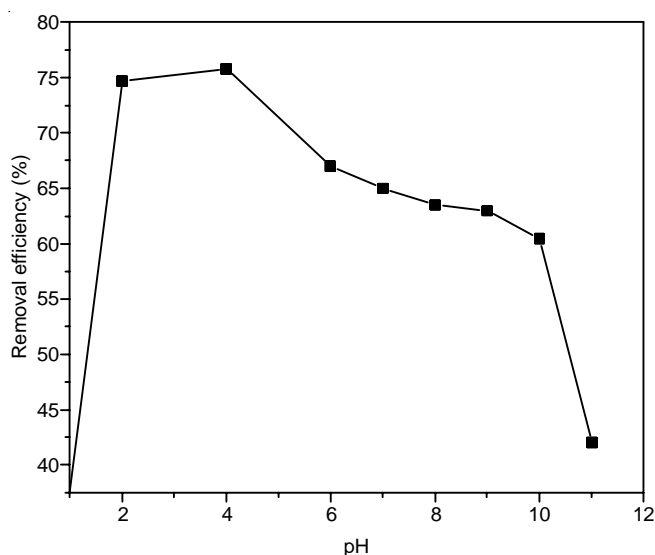


Fig. 7. Effect of pH on adsorption of rhodamine B onto SFTS (adsorbent dose = 0.1 g/50 mL, C = 40 mg/L, t = 80 min)

evident from the figure that the sorption capacity of SFTS decreased from 74.7 to 42.1 % with increase in solution pH 2 to 11. In the present study, it appears that change in pH of solution results in the formation of different ionic species. Below pH 4, rhodamine B ions are of cationic and monomeric molecular form, thus they can enter into pore structure. Above pH 4, the zwitter ionic form of rhodamine B in water may increase the aggregation of rhodamine B to form a dimer and become unable to enter into the pore<sup>19</sup>. This contributes to the decrease in uptake of rhodamine B at higher pH. Similar effect was observed in *Cupressus sempervirens* cones<sup>20</sup>, *Turbinaria conoides*<sup>21</sup> or in *Cypress cone chips*<sup>22</sup>.

**Effect of adsorbent dose:** The effect of SFTS dose on biosorption was studied with 40 mg/L solution and adsorbent dosage ranging from 0.05 to 0.4 g/L. From Fig. 8, it is evident that increase in adsorbent dose increases the dye removal. Increase in dye removal with increase in adsorbent dose was due to the increase of adsorption sites.

**Adsorption isotherm:** Adsorption isotherm models are widely used to describe the adsorption progress and investigate mechanism of adsorption. Adsorption isotherms are basic requirements for the design of adsorption system. Adsorption equilibrium data provide information on the capacity of adsorbent on the amount required to remove a unit mass of pollutant under the system conditions. Langmuir, Freundlich, Temkin and D-R isotherm models were applied to experimental data.

**Langmuir adsorption isotherm:** Langmuir adsorption isotherm has been successfully applied to many adsorption processes and is based on the assumption that adsorption takes place at specific homogeneous sites within the adsorbent. The linearised Langmuir isotherm is represented by the following equation<sup>23</sup>

$$C_e/q_e = 1/Q_0b + C_e/Q_0 \quad (3)$$

where  $C_e$  is the dye concentration at equilibrium (mg/L),  $q_e$  is the adsorption capacity in equilibrium (mg/g),  $b$  is the Langmuir adsorption constant (L/mg) and  $Q_0$  is the maximum adsorption capacity (mg/g).

The essential characteristics of Langmuir adsorption isotherm can be described by means of  $R_L$ , a dimensionless constant referred to as separation factor (or) equilibrium parameter  $R_L$  can be calculated using following equation<sup>24</sup>

$$R_L = 1/(1 + bC_0) \quad (4)$$

where  $C_0$  (mg/L) is the initial concentration of sorbate and  $b$  (mg/L) is the Langmuir constant. The equilibrium parameter  $R_L$  is considered as more reliable indicator of sorption.  $R_L$  value indicates the type of isotherm to be either favorable ( $0 < R_L < 1$ ), unfavorable ( $R_L > 1$ ), linear ( $R_L = 1$ ) or irreversible ( $R_L = 0$ ).

The linear plot of  $C_e/q_e$  versus  $C_e$  (Fig. 9) shows that sorption obeys Langmuir isotherm and the constants  $Q_0$  and  $b$  are evaluated from slope and intercept of the linear plot respectively. The values of  $Q_0$  and  $b$  obtained from slope and intercept of linear plot of  $C_e/q_e$  versus  $C_e$  were found to be 11.63 mg/g and 1.0748 (L/mg) with correlation co-efficient  $R^2$  of 0.998. The  $R_L$  value 0.025 indicates the favorable adsorption of rhodamine B on SFTS.

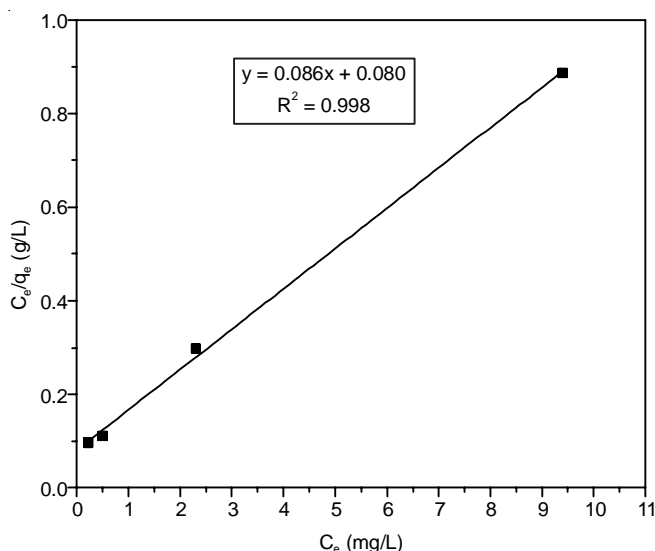


Fig. 9. Langmuir adsorption isotherm for the adsorption of rhodamine B onto SFTS

**Freundlich adsorption isotherm:** Freundlich isotherm model assumes a heterogeneous sorption surface with sites that have different energies of sorption and provides no information on monolayer adsorption capacity.

The linear form of Freundlich adsorption isotherm is represented by following equation<sup>2</sup>.

$$\ln q_e = \ln k_f + 1/n \ln C_e \quad (5)$$

where  $k_f$  is a constant related to sorption capacity (mg/g) and  $1/n$  is an empirical parameter related to sorption intensity. The value of  $n$  varies with heterogeneity of sorbent and gives an idea about the favorability of sorption process. The value of  $n$  should be less than 10 and higher than unity for favorable adsorption. The values of Freundlich constants  $k_f$  and  $1/n$  evaluated from linear plot of  $\ln q_e$  versus  $\ln C_e$  (Fig. 10) were found to be 4.9382 and 0.390 with correlation coefficient  $R^2$  of 0.932.

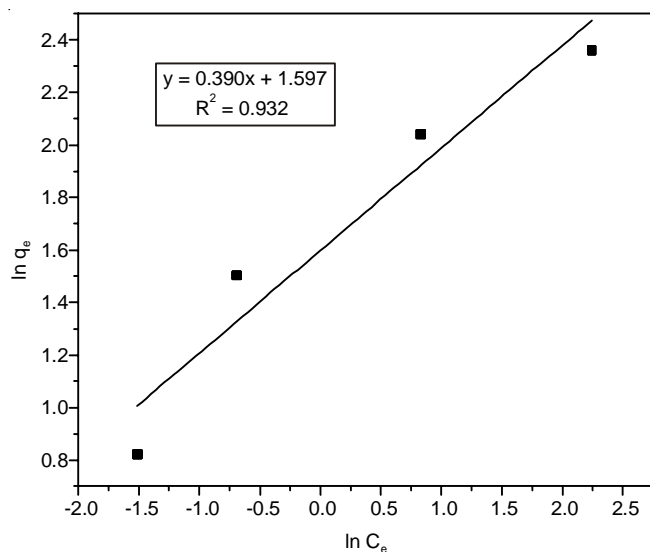


Fig. 10. Freundlich adsorption isotherm for the adsorption of rhodamine B onto SFTS

**Temkin isotherm:** Temkin isotherm contains a factor that clearly indicates the adsorbing species-adsorbate interactions.

The Temkin isotherm assumes that the heat of adsorption of all the molecules in the layer decreases linearly with coverage due to adsorbate - adsorbate interactions and adsorption is characterized by uniform distribution of maximum binding energy. The Temkin isotherm is expressed as<sup>25</sup>

$$q_e = RT/b \ln (K_t C_e) \quad (6)$$

The linear form of Temkin isotherm is expressed as

$$q_e = B_1 \ln K_t + B_1 \ln C_e \quad (7)$$

where  $B_1 = RT/b$ ,  $K_t$  is the equilibrium binding constant (L/mol) corresponding to the maximum binding energy and  $B_1$  is related to heat of adsorption. The above constants are determined using the plot of  $q_e$  vs  $\ln C_e$  (Fig. 11). The values of parameters are presented in Table-2.

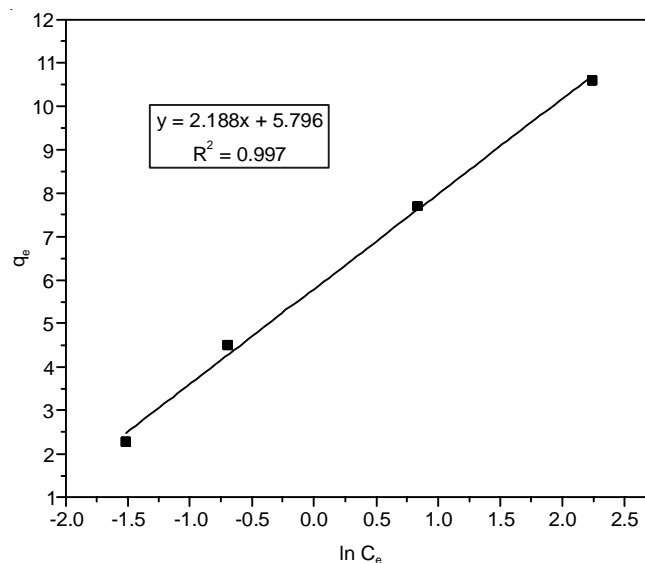


Fig. 11. Temkin isotherm for the adsorption of rhodamine B onto SFTS

TABLE-2  
ISOTHERM PARAMETERS FOR  
ADSORPTION OF RHODAMINE-B ONTO SFTS

Isotherm	Parameters	Values
Langmuir	$Q_0$ (mg/g)	11.63
	$b$ (L/mg <sup>-1</sup> )	1.0748
	$R^2$	0.998
Freundlich	$K_f$ (L/g)	4.9382
	$n$	2.564
	$R^2$	0.932
Temkin	$K_t$ (L/g)	14.139
	$b$ (kJ/mol)	2.188
	$R^2$	0.997
D-R	$Q_m$ (mol/g)	9.057
	$E$ (kJ/mol)	2.5
	$R^2$	0.962

**Dubinin-Radushkevich (D-R) isotherm:** Dubinin-Radushkevich (D-R) isotherm does not assume a homogeneous surface or constant adsorption potential. The linear form of D-R isotherm equation<sup>26</sup> is

$$\ln Q_e = \ln Q_m - \beta \epsilon^2 \quad (8)$$

where  $\beta$  is a constant related to the mean free energy of adsorption per mole of the adsorbate (mol<sup>2</sup> J<sup>-2</sup>),  $Q_m$  is the theoretical saturation capacity (mol/g) and  $\epsilon$  is the polanyi potential.  $\epsilon$ , the polanyi potential can be calculated as follows

$$\epsilon = RT \ln (1 + 1/C_e) \quad (9)$$

where R is the universal gas constant (J/mol/K) and T is the absolute temperature (K). The values of  $Q_m$  and  $\beta$  can be calculated from the intercept and slope of the plot  $\ln Q_e$  vs.  $e^2$ . Values of  $Q_m$  and  $\beta$  were found to be 9.057 (mol/g) and  $4 \times 10^{-4} \text{ mol}^2/\text{J}^2$ , respectively for adsorption of rhodamine B on SFTS. The mean free energy (E) can be calculated using the following relation

$$E = (-2\beta)^{1/2} \tag{10}$$

The mean free energy (E) of adsorption determines the nature of adsorption as physisorption or chemisorption. Physisorption occurs if the value of  $E < 8 \text{ kJ/mol}$  while  $8 < E < 16 \text{ kJ/mol}$  describes chemisorption. The mean free energy (E) calculated were found to be 2.5 kJ/mol which shows that the adsorption of rhodamine B on SFTS is physisorption<sup>27</sup>.

Among the three isotherms, Langmuir adsorption isotherm was found to represent the equilibrium data with a much better fit with high correlation coefficient ( $R^2$ ) 0.998. Table-3 shows the comparison of adsorption capacities ( $Q_0$ ) of various adsorbents for rhodamine B.

Adsorbents	$Q_0$ (mg/g)	References
Simarouba seed shell powder	11.63	This study
Coir pith	2.56	28
Carbonized coir pith	2.6	29
Sago waste carbon	16.2	30
Chemically activated Parthenium biomass	18.52	31
Banana pith	8.5	32
Orange peel	3.2	33
Jute stick powder	87.7	10
Asoka leaf powder	66.6	13
Tannery residual biomass	212.77	34
Dried activated sludge		
Untreated	4.610	
Sulfuric acid treated	7.181	
Hydrochloric treated	6.150	
Sodium hydroxide treated	5.650	35
Sodium montmorillonite	42.19	36
Surfactant modified coir pith	14.90	37

**Adsorption kinetics:** The mechanism of biosorption and potential rate controlling steps such as mass transport and chemical reaction processes can be elucidated by kinetic data of adsorption. Adsorption kinetics was evaluated using pseudo first order, pseudo second order and weber intraparticle models.

**Pseudo first order model:** The linear form of pseudo first order equation can be expressed as<sup>19</sup>

$$\log (q_e - q_t) = \log q_e - (k_1 t)/2.303 \tag{11}$$

where  $q_e$  and  $q_t$  are the sorption capacities at equilibrium time  $t$ , respectively (mg/g) and  $k_1$  ( $\text{min}^{-1}$ ) is the rate constant. The values of  $K_1$  and  $q_e$  were calculated from the slope and intercept of the plot of  $\log (q_e - q_t)$  vs.  $t$  (Fig. 12). Table-4 shows the values of  $q_e$  and  $k_1$  along with the corresponding correlation coefficients for the investigated initial dye concentration. The calculated  $q_e$  were not in good agreement with the experimental  $q_e$  values and the correlation coefficient was found to be relatively low. These observations suggested that pseudo first order is not suitable for biosorption of rhodamine B onto SFTS.

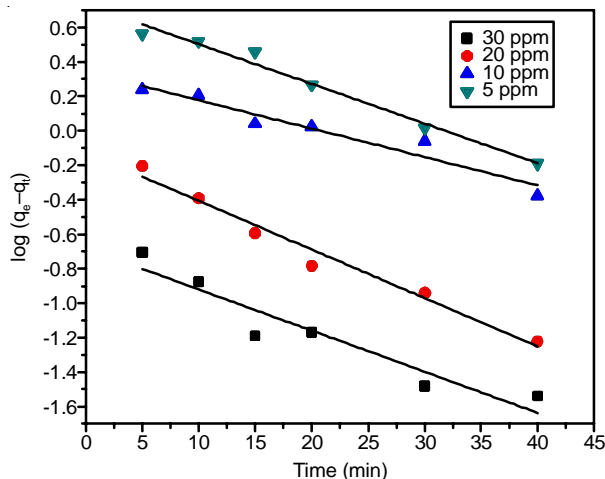


Fig. 12. Pseudo first order plots for the adsorption of rhodamine B onto SFTS

**Pseudo second order model:** The pseudo second order model is based on the assumption that the rate limiting step may be chemisorption involving valence forces through sharing of electrons between sorbent and sorbate as covalent forces.

The pseudo second order model can be represented as<sup>19</sup>

$$t/q_t = 1/k_2 q_e^2 + t/q_e \tag{12}$$

where  $q_e$  and  $q_t$  are the sorption capacities at equilibrium time  $t$ , respectively (mg/g) and  $k_2$  ( $\text{g/mg min}$ ) is the rate constant. Values of  $q_e$  and  $k_2$  were calculated from linear plot of  $t/q_t$  versus  $t$  (Fig. 13) with slope  $1/q_e$  and intercept  $1/k_2 q_e$ . The parameters were presented along with correlation coefficient in Table-4.

The calculated  $q_e$  values agreed well with experimental  $q_e$  with higher correlation coefficient. Thus pseudo second order was predominant and the adsorption was largely controlled by chemisorption process.

**Intraparticle diffusion studies:** The adsorption mechanism of adsorbate onto adsorbent is a multi step process involving transport of solute ions from aqueous phase to the surface of solid particulates and then diffusion of solute ions into the interior of the pores, a slow process and rate deter-

Conc RB (mg/L)	$q_e^{exp}$ (mg/g)	Pseudo first order			Pseudo second order			Intra-particle diffusion	
		$q_e^{cal}$ (mg/g)	$K_1$ ( $\text{min}^{-1}$ )	$R^2$	$q_e^{cal}$ (mg/g)	$K_2$ ( $\text{g/mg min}$ )	$R^2$	$K_{id}$	$R^2$ ( $\text{mg/g min}^{1/2}$ )
5	2.28	0.2089	0.023	0.906	2.294	0.9049	0.999	0.037	0.831
10	4.5	0.7464	0.028	0.975	4.566	0.1934	1	0.111	0.889
20	7.7	2.198	0.016	0.934	7.937	0.039	0.998	0.319	0.929
30	10.6	5.395	0.023	0.979	11.235	0.018	0.998	0.737	0.962

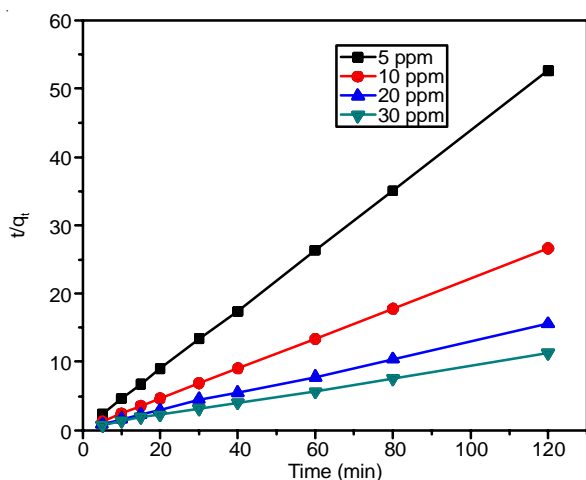


Fig. 13. Pseudo second order plots for the adsorption of rhodamine B onto SFTS

mining<sup>19</sup>. Weber and Morris<sup>38</sup> proposed an empirical relationship that if intraparticle diffusion is rate controlling factor; uptake varies with square root of time. The intraparticle diffusion model is expressed as

$$q_t = K_{id}t^{1/2} + C_i \quad (13)$$

where  $K_{id}$  is intraparticle diffusion constant ( $\text{mg/g min}^{1/2}$ ) and  $C_i$  is the intercept ( $\text{mg/g}$ ). The value of  $K_{id}$  and  $C_i$  can be obtained from the linear plot of  $q_t$  vs.  $t^{1/2}$  (Table-4). Values of  $C_i$  gives an idea about the thickness of boundary layer *i.e* larger the value of  $C_i$  greater the boundary layer effect.

The biosorption of rhodamine B onto SFTS is controlled by intraparticle diffusion if the linear plot of  $q_t$  versus  $t^{1/2}$  is linear and passes through origin. However, the linear plots at each concentration did not pass through origin. This indicates that intraparticle diffusion was not only rate controlling step.

The Boyd model was used to analyse the kinetic data to predict the actual slow step involved in the biosorption process. The Boyd model is expressed as:

$$B_t = -0.4977 - \ln(1-F) \quad (14)$$

where  $F$  represents the fraction of solute adsorbed at any time,  $t$  (min) as calculated using equation

$$F = q_t/q_e \quad (15)$$

Fig. 14 represents the Boyd plot for the adsorption of rhodamine B on SFTS. The figure clearly indicates that the adsorption was mainly governed by film diffusion mechanism as any of the linear plots did not pass through the origin.

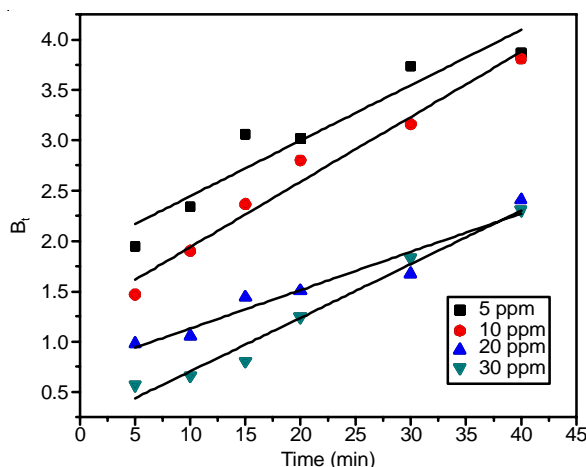


Fig. 14. Boyd plot for adsorption of rhodamine B onto SFTS

## Conclusion

The present study evaluates that the modified seed shell of *Simarouba glauca* can be used as a promising, effective adsorbent for the removal of rhodamine B from wastewater. The adsorption of rhodamine B was found to increase with increase of rhodamine B concentration and contact time. Equilibrium data were best described by Langmuir isotherm with maximum adsorption capacity of 11.63 mg/g. The kinetics of adsorption follows pseudo second order model and the Boyd plot revealed that the adsorption of rhodamine B was controlled by film diffusion.

## REFERENCES

- M.A. Ahmad and R. Alrozi, *Chem. Eng. J.*, **171**, 510 (2011).
- H.B. Senturk, D. Ozdes and C. Duran, *Desalination*, **252**, 81 (2010).
- B.H. Hameed, *J. Hazard. Mater.*, **162**, 939 (2009).
- A. Witek-Krowiak, *Chem. Eng. J.*, **192**, 13 (2012).
- T.S. Anirudhan and P.G. Radhakrishnan, *Desalination*, **249**, 1298 (2009).
- R. Ahmad and R. Kumar, *J. Environ. Manage.*, **91**, 1032 (2010).
- C. Namasivayam and M.V. Sureshkumar, *Bioresour. Technol.*, **99**, 2218 (2008).
- M. Asgher and H.N. Bhatti, *Ecol. Eng.*, **38**, 79 (2012).
- S.D. Khattri and M.K. Singh, *J. Hazard. Mater.*, **167**, 1089 (2009).
- G.C. Panda, S.K. Das and A.K. Guha, *J. Hazard. Mater.*, **164**, 374 (2009).
- R. Dod, G. Banerjee and S. Saini, *Biotechnol. Bioprocess Eng.*, **17**, 862 (2012).
- Z. Zhang, I.M. O'Hara, G.A. Kent and W.O.S. Doherty, *Ind. Crops Prod.*, **42**, 41 (2013).
- N. Gupta, A.K. Kushwaha and M.C. Chattopadhyaya, *J. Taiwan Inst. Chem. Eng.*, **43**, 604 (2012).
- M. Dogan, H. Abak and M. Alkan, *J. Hazard. Mater.*, **164**, 172 (2009).
- D.G. Kinniburgh, J.K. Syers and M.L. Jackson, *Soil Sci. Soc. Am. Proc.*, **39**, 464 (1975).
- S. Benyoucef and M. Amrani, *Desalination*, **275**, 231 (2011).
- K.A. Krishnan and A. Haridas, *J. Hazard. Mater.*, **152**, 527 (2008).
- L. Wang, J. Zhang, R. Zhao, C. Li, Y. Li and C. Zhang, *Desalination*, **254**, 68 (2010).
- H.M.H. Gad and A.A. El-Sayed, *J. Hazard. Mater.*, **168**, 1070 (2009).
- M.E. Fernandez, G.V. Nunell, P.R. Bonelli and A.L. Cukierman, *Bioresour. Technol.*, **101**, 9500 (2010).
- S.L. Hii, S.Y. Yong and C.L. Wong, *J. Appl. Phycol.*, **21**, 625 (2009).
- M.E. Fernandez, G.V. Nunell, P.R. Bonelli and A.L. Cukierman, *Bioresour. Technol.*, **106**, 55 (2012).
- X. Xue, X. He and Y. Zhao, *Desalin. Water Treat.*, **37**, 259 (2012).
- C. Namasivayam and R.T. Yamuna, *Water Air Soil Pollut.*, **113**, 371 (1999).
- D. Kavitha and C. Namasivayam, *Bioresour. Technol.*, **98**, 14 (2007).
- H. El Bakouri, J. Usero, J. Morillo and A. Ouassini, *Bioresour. Technol.*, **100**, 4147 (2009).
- V.K. Gupta, M.R. Ganjali, A. Nayak, B. Bhushan and S. Agarwal, *Chem. Eng. J.*, **197**, 330 (2012).
- C. Namasivayam, K.D. Kumar, R. Selvi, T.A. Begum, T. Vanathi and R.T. Yamuna, *Biomass Bioenergy*, **21**, 477 (2001).
- C. Namasivayam, R. Radhika and S. Suba, *Waste Manage.*, **21**, 381 (2001).
- K. Kadirvelu, C. Karthika, N. Vennilamani and S. Pattabhi, *Chemosphere*, **60**, 1009 (2005).
- H. Lata, V.K. Garg and R.K. Gupta, *Desalination*, **219**, 250 (2008).
- C. Namasivayam, N. Kanchana and R.T. Yamuna, *Waste Manage.*, **13**, 89 (1993).
- C. Namasivayam, N. Muniasamy, K. Gayatri, M. Rani and K. Ranganathan, *Bioresour. Technol.*, **57**, 37 (1996).
- J. Anandkumar and B. Mandal, *J. Hazard. Mater.*, **186**, 1088 (2011).
- D.J. Ju, I.G. Byun, J.J. Park, C.H. Lee, G.H. Ahn and T.J. Park, *Bioresour. Technol.*, **99**, 7971 (2008).
- P.P. Selvam, S. Preethi, P. Basakaralingam, N. Thinakaran, A. Sivasamy and S. Sivanesan, *J. Hazard. Mater.*, **155**, 39 (2008).
- M.V. Sureshkumar and C. Namasivayam, *Colloids Surf. A Physicochem. Eng. Asp.*, **317**, 277 (2008).
- W.J. Weber and J.C. Morris, *Advances in Water Pollution Research: Removal of Biologically Resistant Pollutants from Waste Waters by Adsorption*. In: Proceedings of the International Conference on Water Pollution Symposium, Pergamon Press, Oxford, vol. 2 (1962).